IDENTIFICATION AND VERIFICATION OF TERMINATION CONDITIONS IN FINE MOTION IN PRESENCE OF SENSOR ERRORS AND GEOMETRIC UNCERTAINTIES

Rajiv S. Desai
Jet Propulsion Laboratory
California Institute Of Technology
Pasadena, California 91109

Richard A. Volz
Department of Computer Science
Texas A & M University
College Station, Texas 77843

Dear Professor Volz:

In 1984, I was a starry eyed student in mechanical engineering who liked making robots. Although you were in the electrical engineering department, you took me under your wings and gave me a chance to learn and grow. Your patience and persistence helped me finish my thesis. Your introducing me to NASA changed my life. I have had an extremely fulfilling career. I feel privileged to have been your student. I shall always be deeply indebted to you.

Thank you.

Sincerely,

Rajiv Desai

गुरु = Guru = Teacher/Mentor

In Sanskrit gu means darkness & ru means light.

A guru (Sanskrit: गुरु) is one who is regarded as having great knowledge, wisdom and authority in a certain area, and who uses it to guide others (teacher).

शिष्य = Shishya = Student/Disciple

The Guru-Shishya tradition:
The ancient Hindu tradition of transmission of teachings from the teacher to disciple, known as the Guru-Shishya (गुरु - शिष्य) tradition goes back to 2000 B.C.

In this relationship, subtle and advanced knowledge is conveyed and received through the student's respect, commitment, devotion and obedience. The student eventually masters the knowledge that the guru embodies.

गुरु गोविन्द दोऊ खड़े काको लागूं पायं।
बलिहारी गुरु आपने जिन गोविन्द दियो बताय।।
(Kabir, c 1450 AD)

My teacher and God both stand before me, who should I pay respects to first?
I bow to thee first my teacher, for you showed me the way to God (Knowledge).

1989 IEEE International Conference on Robotics and Automation,
May 14-19, 1989, Scottsdale, AZ, United States

IDENTIFICATION AND VERIFICATION OF TERMINATION CONDITIONS IN FINE MOTION IN PRESENCE OF SENSOR ERRORS AND GEOMETRIC UNCERTAINTIES

Rajiv S. Desai
Jet Propulsion Laboratory
California Institute Of Technology
Pasadena, California 91109

Richard A. Volz
Department of Computer Science
Texas A & M University
College Station, Texas 77843

Abstract

In order to achieve an ultimate goal of automatically generating assembly programs for robots from design information, it is necessary that one be able to devise part-mating strategies that will work in spite of sensor, control and manufacturing errors. In general, this is almost certainly unachievable. Typically, part mating strategies consist of sequence of guarded or compliant guarded motions. It is important to be able to *verify*, both succesful and unsuccessful, termination of these motion. Moreover, it is important to *identify* the termination state at the end of these guarded motions.

As the first step in our approach, we introduce a concept of *contact formations* to describe contacts among parts in a system, aiming at reducing the dimensionality of assembly verification. We also describe a technique for identifying contact formations in spite of errors in sensing and geometric uncertainties. It is impossible to verify termination conditions in general. Notion of design constraints is introduced and design constraints for for which verification can be guaranteed are formulated. The constraints are reasonable in the sense that they do not impose unrealistic conditions on typical designs. Results of implementation on a robot system consiting of a PUMA robot with RTI force/torque sensors uphold the theoretical derivations and show empirically that the theoretical constraints can be relaxed somewhat with good results still obtained.

1 Introduction

The manual development of robot programs for assembly is a laborious, error prone task. It would be highly desirable to be able to derive such programs automatically from design information. In order to do so, a key problem is to transfer a given sequence of assembly operations into executable robot motion plans. The problem leads to the following subproblems 1) gross motion planning [2] [3][4], 2) grasp planning [5] [7] [8] [9], and 3) fine motion planning with uncertainty handling. This paper addresses the last of these subproblems.

It has often been stated that the largest part of any robot assembly program consists of fix-ups to handle things that don't quite work as planned [10]. Algorithms for generating these fix-ups are crucial to successful automatic program generation. Problems in the execution of nominal robot programs arise due to control errors, sensing errors and modelling (geometric) errors (tolerances).

Often such errors can lead to the failure of a nominal program that would theoretically accomplish a task such as part mating. The automatic generation of robot programs for assembly cannot be successful until some means of either avoiding or correcting these errors is found.

Several approaches towards handling these uncertainties have appeared in the literature. Taylor[11] introduced an error-propagation method to estimate compound errors from the uncertainty bound or tolerance of each individual part (including the robot hand) involved in a task. Brooks[12] extended Taylor's method by making the process reversible, so that the constraints on some compound errors to make the task succeed can lead to constraints on individual parts. This method, however, suffers from high computational complexity. And, it does not provide means to reduce errors dynamically. The inductive learning approach by Dufay and Latombe[13] corrects run-time errors by adding rules into the system as a corrective plan. In this approach, error-handling is not fully automatic since rules must be provided by human users.

The pre-image approach introduced by Lozano-Pérez, Mason, and Taylor[14][15], and simplified by Erdmann [16] incorporates the effect of uncertainty directly within one planning phase. The goal is to create motion plans that will avoid errors. However, this approach has unsolved theoretical problems. Donald[17] also developed an error detection and recovery strategy based on preimages.

Most of the fine motion approaches use both position and force control[18][19] [20] [21] of the manipulator, for reducing errors and uncertainties that pure positioning control is incapable of. A practical force control method was developed by Whitney[22]. His remote center compliance(RCC) device can correct small insertion errors for a peg-in-hole task by applying correct forces/torques to the peg, but it only works when the peg is in or partly in the hole.

A different approach focuses on devising sensorless motion strategies to reduce errors [6][24][25]. However, this approach can only be applied to limited tasks. It can not be used for tasks with tight tolerances, such as high precision insertion tasks.

All the previous approaches contribute to solving the problem in some ways, but none fully solve it. The problem is very complex, and new approaches are needed. We present algorithms for robotic assembly based upon these principles and the use of *imperfect* position, force, moment and contact sensors in the presence of control errors. Yet, the algorithms can be shown to be successful in spite of certain classes of sensor, control and manufacturing imperfections.

We utilize a two phase planning process, consisting of an off-line nominal planner and an on-line replanner to correct run-time errors. The nominal plan is defined as a sequence of robot motions to complete a part-mating task *without taking into account the effect of uncertainty*. A nominal plan will guide the robot to act correctly if no errors are present, but the action may fail to meet the desired goal in reality because there will always be some uncertainty, i.e., errors may occur. We presume that the nominal planner already exists, and propose to concentrate on developing replanning algorithms for the robot motion to correct errors and resume the nominal plan. As contact is obviously involved, we also assume the existence of compliant motion controllers [26] and focus on developing the commands to such controllers.

The system framework relevant to the proposed approach consists of three components: a verifier, a replanner, and an executor. Given the task environment(i.e. the robot, the assembly parts, and the sensors), a nominal plan consisting of guarded and compliant guarded motions, and a world model which consists of geometrical and physical descriptions of the task environment, the executor executes a guarded motion from the nominal plan. The verifier identifies contact state among the assembly parts at the termination of each guarded motion. If the termination state at the end the motion, as identified by the verifier is different from the expected termination state, then the replanner generates patch-plans to correct errors. Each patch-plan generates a path connecting the unexpected configuration to one from which the nominal control can continue.

The major steps in our approach are, description and classification of contacts, modeling of sensing and geomtric uncertainties, development of identification and verification algorithms and determination of design constraints for which the algorithms are guaranteed to work.

CH2750-8/89/0000/0800$01.00 © 1989 IEEE

Problems of nominal planning and replanning are not discussed in this paper.

Error Models

For successful verification and replanning, it is necessary to establish an appropriate error model which describes all (dominant) static errors in a system. Dynamic errors such as the control errors are not relevant to the verification problem because the verification is performed after a guarded (or a compliant guarded) motion has terminated. We suppose that both a position/orientation sensor and a force/torque sensor are available. Then the geometric uncertainties and uncertainties in position (orientation) and force (torque) sensing must be modeled.

2.1 Geometric Modeling Uncertainty

Let, $\mathbf{P}_a$ denote the actual position of a point on an object, and $\mathbf{P}_m$ denote the corresponding modelled value for the position of that point.

Definition 1: γ_p is defined as *geometric uncertainty* in position, iff $\gamma_p > 0$, and $\forall \mathbf{P}_a$, $\forall \mathbf{P}_m$, if $\mathbf{P}_a$ is the actual position and $\mathbf{P}_m$ is the modelled position. Then,

$$\|\mathbf{P}_a - \mathbf{P}_m\| < \gamma_p.$$

Similarly, we define the geometric uncertainty in orientation γ_n. Let, $\mathbf{N}_a$ denote the actual surface normal at any point on an object, and $\mathbf{N}_m$ denote the corresponding modelled value for the surface normal at that point.

Definition 2: ϵ_n is defined as *geometric uncertainty* in orientation, iff $\gamma_n > 0$, and $\forall \mathbf{N}_a$, $\forall \mathbf{N}_m$, if $\mathbf{N}_a$ is the actual orientation and $\mathbf{N}_m$ is the modelled orientation. Then,

$$\|\mathbf{N}_a \cdot \mathbf{N}_m\| > \gamma_n.$$

2.2 Modeling Position/Orientation Sensor Uncertainty

Let $(\mathbf{P}_a, \phi_a)$ denote a location in the system configuration space constrained by the Compliant Surface (C-Surface), where $\mathbf{P}_a$ refers to the position and ϕ_a refers to the orientation. Let $(\mathbf{P}_s, \phi_s)$ denote the corresponding sensed position and orientation on a position/orientation sensor.

Definition 3: ϵ_p is defined as the *positional uncertainty* of a position/orientation sensor, iff $\epsilon_p > 0$, and it has the smallest value satisfying the condition that $\forall \mathbf{P}_a$, $\forall \mathbf{P}_s$, if $\mathbf{P}_a$ is sensed by the position/orientation sensor as $\mathbf{P}_s$, then

$$\|\mathbf{P}_s - \mathbf{P}_a\| \leq \epsilon_p.$$

In actuality there are two position errors of concern when we are dealing with two objects being mated, one for each object. Typically one object will be held by the robot hand and one will be fixtured. We use similar models for both but with different error bounds. We use ϵ_{pl} for the bound on the fixtured object and ϵ_p for the object held in the robot hand.

Definition 4: ϵ_o is defined as the *orientational uncertainty* of a position/orientation sensor, iff $\epsilon_o > 0$, and it has the smallest value satisfying the condition that $\forall \phi_a$, $\forall \phi_s$, if ϕ_a is sensed by the position/orientation sensor as ϕ_s, then

$$\|\phi_s - \phi_a\| \leq \epsilon_o.$$

2.3 Modeling Force/Torque Sensor Uncertainty

Let $\mathbf{F}_s$ denote a force sensed by a force/torque sensor. Let $\mathbf{F}_a$ be the actual force.

Definition 5: ϵ_f is defined as the *force uncertainty* of a force/torque sensor , iff $\epsilon_f > 0$, and it has the smallest value satisfying the condition that $\forall \mathbf{F}_a$, $\forall \mathbf{F}_s$, if $\mathbf{F}_a$ is sensed by the position/orientation sensor as $\mathbf{F}_s$, then

$$\|\mathbf{F}_s - \mathbf{F}_a\| \leq \epsilon_f.$$

Let $\mathbf{M}_s$ denote a moment sensed by a force/torque sensor. Let $\mathbf{M}_a$ be the actual moment.

Definition 6: ϵ_m is defined as the *momental uncertainty* of a force/torque sensor , iff $\epsilon_m > 0$, and it has the smallest value satisfying the condition that $\forall \mathbf{M}_a$, $\forall \mathbf{M}_s$, if $\mathbf{M}_a$ is sensed by the position/orientation sensor as $\mathbf{M}_s$, then

$$\|\mathbf{M}_s - \mathbf{M}_a\| \leq \epsilon_m.$$

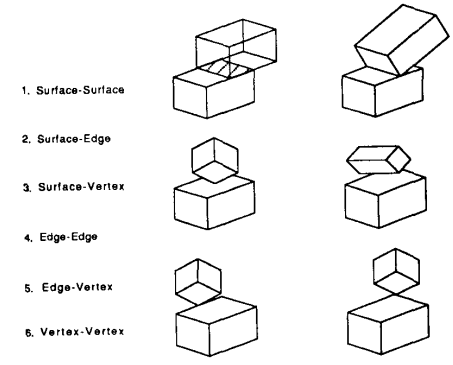

Figure 1: Elemental contacts

3 Contact Formations—A New Way to Describe and Classify Contacts

The exterior of a solid part is known to consist of three topological elements, surfaces, edges and vertices. One of the principles upon which we build our approach is that when two objects are in contact (one fixtured and one held by the robot), the structure (kind) of control we use is determined by *how* the objects contact each other topologically, not their precise relative pose (i.e., position and orientation). That is, the control structure will be variable depending upon nature of the topological contacts among the parts involved. Individual coefficients in the control algorithms, though, may be dependent upon the (imperfect) readings of sensors in the system. We thus seek methods for identifying the kind of topological contact present as a first step in our approach.

Our second principle is that design constraints are necessary for being able to assure that our approach will work. We will show that these constraints are necessary both to identify the type of contact and to ensure that the corresponding controls will work in spite of errors present.

3.1 Contact Formations–Definition

In this section, we introduce a means to describe and classify contacts between a set of parts. Usually, there are an infinite number of relative locations that have the same topological contacts among the elements of the parts. We introduce the concept of Contact Formations used to classify contacts based on toplogical similarity.

The position and orientation of a rigid body can be specified by a six-dimensional vector, called it's *configuration*. The six-dimensional space of configurations for a body, i, is called its *configuration space* and denoted by $C - Space_i$. More generally, a system of objects in

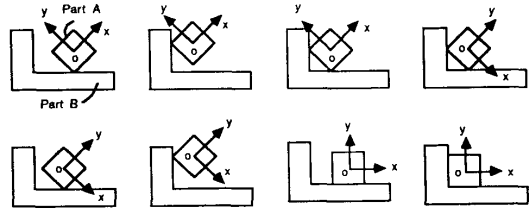

Figure 2: Contact formations

which position and orientation of each object can be specified by a

total n parameters can be modelled by a n-dimensional configuration space. We define an elemental contact between two objects i and j as being a contact between any two topological elements of the objects (see Fig. 1). An elemental contact between topological element e_i^l of object i and topological element e_j^k of object j is represented as a pair $\{e_i^l, e_j^k\}$. We assume that a topological element includes its interior but not it's bounding elements, i.e., it is open. For example, an edge of a polyhedron does not include the two vertices bounding it, and a face does not include the edges (and therefore vertices) bounding it.

We define a *contact formation* as the set of all configurations, with identical elemental contacts between the same pairs of topological elements (For an example, see Fig. 2). We can also view a contact formation between objects i and j as a set of elemental contacts, $CF = \{.., \{e_i^l, e_j^k\}, ..\}$. Configurations for which there is no contact among objects, are said to be in free space. For a detailed development of the concept of Contact Formations, refer to Desai[29].

We can state the fine motion planning problem in terms of contact formation. Our goal state is to achieve a certain (set of) contact formations between the objects involved and to satisfy certain positional/orientation constraints. Contact formations are thus one part of the goal we must satisfy. Now, one can think of part mating as first moving from an initial contact formation to goal contact formation. Consider the example of the peg in the hole problem as shown in Fig. 3. The assembly plan is shown as a path going though several contact formations from start to finish. For each move from one contact formation to its neighbor, a second level planning step is required to generate a motion within a single contact formation. In this case, the planning problem is reduced in dimensionality. Further, we expect that because the replanned motion must only be to a neighboring contact formation, some simple algorithm for the motion, e.g., straight line or simple rotation will be possible.

3.2 Contact Analysis

The objective of the verifier is to identify the contact formation in which a motion terminates. Verification is done in two phases, a *passive* (or static) phase and if necessary, an *active* phase. In passive verification, the contact formation is identified on the basis of the sensed data[1] by formulating a hypothesis regarding the contact condition and verifying if it is consistent with the sensed data. This requires solving for contact forces and moments. Unfortunately it is not always possible to determine the contact forces and moments. Moreover, even when contact forces and moments can be determined, it is not always possible to disambiguate all contact formations due to sensing and geometric uncertainties and approximation of the contact model used.

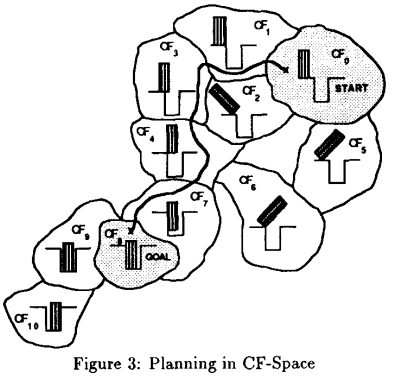

Figure 3: Planning in CF-Space

When passive verification does not succeed in identifying a contact formation, *active* verification is used. In active verification more information about the contact formation is collected by making small moves using a new concept of *separation cones*.

[1] Sensed position, forces and moments

3.2.1 The Contact Model

An unconstrained rigid polyhedral body $\mathbf{B}$ in space has six degrees of freedom. Henceforth, $\mathbf{B}$ will always refer to the object held in the gripper, unless stated otherwise. Now, suppose there exists another body $\mathbf{B}'$ in space, such that $\mathbf{B}$ and $\mathbf{B}'$ are in contact. There are six types of *elemental contacts* that can theoretically take place between two polyhedral objects. However, only four occur in reality.

We define a *contact normal* (a unit vector, $\hat{\mathbf{n}}_c$) for each type of elemental contacts. For each of the first three cases, *Face-Face contact*, *Edge-Face contact* and, *Vertex-Face contact* $\hat{\mathbf{n}}_c$ is defined by the outward normal of the face in contact (outward to $\mathbf{B}$ in face-face case). The only *Edge-Edge contact* that is of interest is when the two edges are not parallel. In such case $\hat{\mathbf{n}}_c$ is defined by the normal of the plane containing both those edges, outward from $\mathbf{B}$.

The plane containing the elemental contact and described by the contact normal $\hat{\mathbf{n}}_c$ is called the *contact plane* for that elemental contact. A *Contact Frame of Reference* can be defined for each type of elemental contact by three mutually orthogonal unit vectors $\hat{\mathbf{n}}_x$ $\hat{\mathbf{n}}_y$ and $\hat{\mathbf{n}}_z$, such that $\hat{\mathbf{n}}_z$ is along the contact normal $\hat{\mathbf{n}}_c$ and $\hat{\mathbf{n}}_x$ $\hat{\mathbf{n}}_y$ lie in the contact plane[2]. The origin of the *Contact Frame of Reference* o_c lies at the centroid of the contact area[3]

All contacts except the point contacts, i.e., Vertex-Face and Edge-Edge Contacts, are referred to as *distributed* contacts. We assume that the objects are rigid everywhere except close to the contact surface, i.e., the deformation due to contact is localized around the actual contact surface. The contact surface is denoted by S.

The normal pressure acting on $\mathbf{B}$ at (x, y) is given by the *Contact Pressure Distribution*, $P(x, y)$. Suppose that the relative velocity between point (x, y) on $\mathbf{B}$ and the corresponding point on $\mathbf{B}'$ is $v(x, y)$, and magnitude of the traction due to friction at (x, y) is $f(x, y)$. Then,

$$f(x,y) < \mu(x,y)P(x,y) \quad \text{for sticking, and} \tag{1}$$

$$f(x,y) = \mu(x,y)P(x,y) \qquad \text{for slipping} \tag{2}$$

For line contact, the *Pressure Distribution*, relative velocity function and magnitude of traction due to friction are denoted by $P(l)$[4], $v(l)$ and $f(l)$, respectively, where l is a parameter along the line of contact. For case of a point contact, only contact force $\mathbf{F}$ and relative velocity $\mathbf{v}$, are relevant.

3.2.2 Static Equilibrium Equations

Let $\mathbf{N}_c$ be the total number elemental contacts between $\mathbf{B}$ and $\mathbf{B}'$, and, $\mathbf{N}_s$ $\mathbf{N}_l$ $\mathbf{N}_p$, the number of planar, line and point contacts. Then,

$$N_c = N_s + N_l + N_p \tag{3}$$

and the equations for static equilibrium are:

$$\begin{aligned} &\sum_{i=1}^{N_p} \mathbf{F}_i + \sum_{i=1}^{N_l} \int_{L_i} \left(P_{l,i}(l)\hat{\mathbf{n}}_{i,z} - f_{l,i}(l)\frac{\mathbf{v}_{l,i}(l)}{|\mathbf{v}_{l,i}(l)|} \right) dl \\ &+ \sum_{i=1}^{N_s} \int_{A_i} \left(P_{s,i}(x,y)\hat{\mathbf{n}}_{i,z} - f_{s,i}(x,y)\frac{\mathbf{v}_{s,i}(x,y)}{|\mathbf{v}_{s,i}(x,y)|} \right) dxdy + \mathbf{F}_b + \mathbf{F}_e = 0 \end{aligned} \tag{4}$$

$$\begin{aligned} &\sum_{i=1}^{N_l} \int_{L_i} \left(\left[\mathbf{r}_{l,i}^{o_c} + \mathbf{r}'_{l,i}(l) \right] \otimes \left[P_{l,i}(l)\hat{\mathbf{n}}_{i,z} - f_{l,i}(l)\frac{\mathbf{v}_{l,i}(l)}{|\mathbf{v}_{l,i}(l)|} \right] \right) dl \\ &+ \sum_{i=1}^{N_s} \int_{A_i} \left(\left[\mathbf{r}_{s,i}^{o_c} + \mathbf{r}'_{s,i}(x,y) \right] \otimes \left[P_{s,i}(x,y)\hat{\mathbf{n}}_{i,z} - f_{s,i}(x,y)\frac{\mathbf{v}_{s,i}(x,y)}{|\mathbf{v}_{s,i}(x,y)|} \right] \right) \\ &+ \sum_{i=1}^{N_p} (\mathbf{r}_i \otimes \mathbf{F}_i) + \mathbf{r}_b \otimes \mathbf{F}_b + \mathbf{M}_e = 0 \end{aligned} \tag{5}$$

where:

[2] In case of a line contact, $\hat{\mathbf{n}}_x$ is chosen to lie along the line of contact

[3] In case of a point contact o_c lies at the point of contact, and, for line contact o_c lies at the midpoint of the line segment along which the contact occurs.

[4] $P(l)$ has the units of Force/Length

$\mathbf{N}_c$	=	Total number of Elemental Contacts
$\mathbf{N}_p$	=	Number of point contacts
$\mathbf{N}_l$	=	Number of line contacts
$\mathbf{N}_s$	=	Number of planar contacts
$f_{l,k}(l)$	=	Magnitude of traction due to friction i^{th} line contact.
$f_{s,i}(x,y)$	=	Magnitude of traction due to friction i^{th} planar contact.
$\mathbf{v}_{l,i}(l)$	=	Relative velocity function i^{th} line contact.
$\mathbf{v}_{s,i}(x,y)$	=	Relative velocity function i^{th} planar contact.
$P_{l,i}(l)$	=	Normal pressure distribution function for i^{th} line contact.
$P_{s,i}(x,y)$	=	Normal pressure distribution function for i^{th} planar contact
$\mathbf{r}^{o_c}_{l,i}$	=	Position vector to the origin of i^{th} *Contact Frame of Reference* for a line contact
$\mathbf{r}^{o_c}_{s,i}$	=	Position vector to the origin of i^{th} *Contact Frame of Reference* for a planar contact
$\mathbf{r'}_{l,i}(l)$	=	Position vector of point on i^{th} line contact in i^{th} *Contact Frame of Reference*
$\mathbf{r'}_{s,i}(x,y)$	=	Position vector of point (x,y) on i^{th} contact surface in i^{th} *Contact Frame of Reference.*
$\mathbf{r}_b$	=	Position vector of the point where $\mathbf{F}_b$ is applied
μ	=	Coefficient of friction
$\mathbf{F}_i$	=	Contact Force at i^{th} point contact.
$\mathbf{F}_e$	=	External Force
$\mathbf{F}_b$	=	Body Force (weight of object)
$\mathbf{M}_e$	=	External Moment

Our immediate objective is to determine the contact pressure distributions $\mathbf{P}_{l,i}(l)$ and $\mathbf{P}_{a,i}(x,y)$ and contact forces $\mathbf{F}_i$. In general these equations are insufficient as number of unknowns is greater than the number of equations. For the case of negligible friction, Kalker[27] discusses several variational formulations that are extant. Torigaki and Kikucki[28] have done a Finite Element Analysis of a class of contact problems with multiple contacts with friction, by using a penalty method and regularization function to approximate the variational inequality representing the principle of virtual work associated with friction contact problem. However, all these methods are computationally too expensive and presently unsuitable.

By assuming that the contact pressure is uniform over the contact area, the equilibrium equations are simplified. Then, $\mathbf{P}_{s,i}(x,y) = \mathbf{P}_{s,i}$ and $\mathbf{P}_{l,i}(l) = \mathbf{P}_{l,i}$, where $\mathbf{P}_{s,i}$ and $\mathbf{P}_{l,i}$ are constants. It can be shown that uniform pressure assumption is equivalent to a force acting through the centroid of the contact area. For the i^{th} distributed contact, let that force be $\mathbf{F}_i$. The only moment that can be transmitted through a uniformly distributed contact is the moment about the contact normal $\mathbf{n}_c$. Therefore, the effect of the i^{th} uniformly distributed contact can be replaced by a contact wrench $\mathbf{w}_i = (\mathbf{F}_i, \mathbf{M}_i)^T$, where $\mathbf{F}_i$ and $\mathbf{M}_i$ are contact force and moment transmitted at the centroid o_c. Then, the static equilibrium equations can be rewritten as,

$$\sum_{i=1}^{\mathbf{N}_c} \mathbf{F}_i + \mathbf{F}_b = -\mathbf{F}_e \tag{6}$$

$$\sum_{i=1}^{\mathbf{N}_c} (\mathbf{r}_i \bigotimes \mathbf{F}_i + \mathbf{M}_i) + \mathbf{r}_b \bigotimes \mathbf{F}_b = -\mathbf{M}_e \tag{7}$$

In *statically determinate systems,* where there are at least as many independent equilibrium equations as there are unknown forces and moments it is possible to determine all contact forces from static equilibrium equations for the contacting objects. This is true of cases where there is only a single contact present, i.e., $\mathbf{N}_c = 1$.

3.2.3 Single Contact ($\mathbf{N}_c = 1$ case)

The case of single contact is an important one that will be directly used in verification. In this case the equilibrium equations further simplify to:

$$\mathbf{F}_c + \mathbf{F}_b = -\mathbf{F}_e \tag{8}$$

$$\mathbf{r}_c \bigotimes \mathbf{F}_c + \mathbf{M}_c + \mathbf{r}_b \bigotimes \mathbf{F}_b = -\mathbf{M}_e \tag{9}$$

where, $\mathbf{F}_c$, $\mathbf{r}_c$ and $\mathbf{M}_c$ are the contact force, location of the centroid of the contact surface, and moment transmitted through the contact, respectively. The contact loads, $\mathbf{F}_c$ and $\mathbf{M}_c$ are easily determined from above equations[5].

3.2.4 Multiple Contacts

Multiple contacts also occur quite frequently in assembly. However, in general, multiple contact situations are statically indeterminate, and the equilibrium equations are insufficient to determine the contact forces and moments. Desai[29] derives a potential energy and virtual displacement method for estimating contact forces for multiple contacts. Due to limitation of space, however the argument will not be presented here.

3.2.5 Geometric Analysis of Contacts As we shall see static equilibrium equation are not always sufficient for verification. For the remaining cases, a geometric analysis is useful. The condition of contact between two objects from the perspective of geometry can be viewed as a constraint on the motion of one object with respect to other. We define two types of translation motion, namely, *separation motion* and *compliant motion.* Any differential motion that results in breaking the contact between the objects is termed *separation motion.* Any differential motion that does not result in breaking of contact is termed *compliant motion.* Clearly, all the permissible differential motions for rigid bodies are either *separation motions* or *compliant motions.* Then, the *separation cone* of a contact is defined as the set of all *separation motions* for that contact. Similarly, the *compliant cone* is defined as the set of all the compliant motions for that contact. Now we generalize the concept of *separation cones* to contact formations.

Separation Cones for Elemental Contacts

All *Elemental Contacts* among polyhedral objects are either point, linear or planar contacts. First, we define Separation Cones for each type of Elemental Contact and then extend the idea to Contact Formations.

Vertex-Face and *Nonparallel Edge-Edge.* The separation cone for these cases is determined by the *contact plane* for the contact.

Edge-Face: The motion of a line (or a line segment) is completely specified by motion of two non-coincident points on that line. An Edge-Face contact may occur over several disconnected segments. However, each segment is bounded by either a Vertex-Face or Edge-Edge Contact. Thus, if $S_{s_1}, S_{s_2} \ldots S_{s_n}$ are the Separation Cones for the n edge segments, then Separation Cone for the Edge-Face contact is computed by,

$$S_{ef} = \bigcap_{i=1}^{n} S_{s_i} \tag{10}$$

where, S_{s_i} are computed by,

$$S_{s_i} = S_{i_1} \bigcap S_{i_2} \tag{11}$$

and S_{i_1} and S_{i_2} are the Separation Cones for bounding Elemental Contacts, which are either Edge-Edge or Vertex-Face.

Face-Face: The motion of a plane is specified by specifying the motion of any three non-colinear points on that plane. In general, a Face-Face contact may consist of several disconnected regions of contact. Each such disconnected region of Face-Face Elemental Contact is bounded by either a Vertex-Face, Edge-Edge or Edge-Face Elemental Contact. Now, if $S_{r_1}, S_{r_2} \ldots S_{r_n}$ are Separation Cones for the n disconnected regions of Face-Face Elemental Contact, then, the Separation Cone for a Face-Face Elemental Contact is given by,

$$S_{ff} = \bigcap_{i=1}^{n} S_{r_i} \tag{12}$$

[5]The direction of the moment vector is known; only the magnitude needs to be determined.

where, S_{r_i} is given by,

$$S_{r_i} = \bigcap_{j=1}^{m} S_{i_j} \tag{13}$$

and, S_{i_j} are Separation Cones for bounding Vertex-Face, Edge-Edge, and Edge-Face Elemental Contacts of region r_i.

Separation Cones for Contact Formations

A Contact Formation is a set of Elemental Contacts. A Separation Cone for a Contact Formation is defined as a set of all the differential straightline motions that result in a breaking of *all* the elemental contacts. Suppose there are l elemental contacts in a Contact Formation, and let S_k denote the separation cone for k^{th} elemental contact. Then, Separation Cone, S_{cf} for the contact formation is given by,

$$S_{cf} = \bigcap_{k=1}^{l} S_k \tag{14}$$

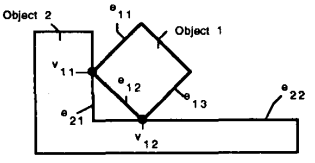

Figure 4: A Contact Formation

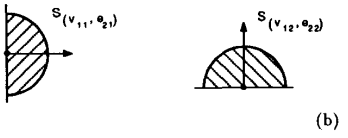

Figure 5: Separation Cones for Elemental Contacts (a) $\{v_1, e_4\}$, (b) $\{v_2, e_5\}$, of the Contact Formation shown in Fig.7.

For example, consider the contact formation shown in Fig. 4. There are six elemental contacts in this contact formation, namely, $\{e_{11}, e_{21}\}$, $\{e_{12}, e_{21}\}$, $\{e_{12}, e_{22}\}$, $\{e_{13}, e_{22}\}$, $\{v_{11}, e_{21}\}$ and $\{v_{12}, e_{22}\}$. As we mentioned above, only the vertex contacts need to be considered to compute the separation cone. Fig. 5(a) and Fig. 5(b) show the separation cones $S_{\{v_1,e_4\}}$ and $S_{\{v_2,e_5\}}$ for Elemental Contacts $\{v_1, e_4\}$ and $\{v_2, e_5\}$ respectively. Then, the separation cone for the contact formation is computed as follows:

$$S_{CF} = S_{\{v_{11},e_{21}\}} \bigcap S_{\{v_{12},e_{22}\}} \tag{15}$$

The Separation Cone for the Contact Formation in Fig. 4 is shown in Fig. 6.

3.3 The Verification Algorithm

The previous section has developed the tools needed for the verification algorithm to identify the contact formation in which a guarded

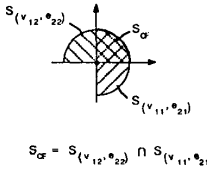

Figure 6: Separation Cone for Contact Formation shown in Fig.7.

motion terminates. Verification is done in two phases, a *passive* (or *static*) verification phase and *active* verification phase. Both verification algorithms are based on a hypothesis and test scheme. In the *static* contact formations are tested by formulating a hypothesis regarding the

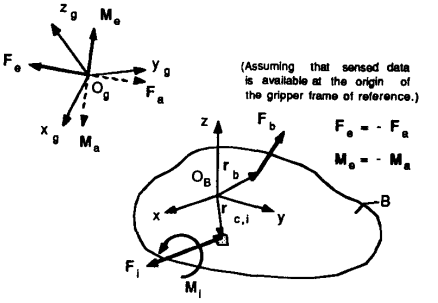

Figure 7: Sensed Forces

contact condition and verifying whether or not this is consistent with the sensed data. The *active* verification phase is used only if the static verification phase does not succeed in uniquely identifying the Contact Formation, and is based upon the separation cones.

3.3.1 Static Verification

Let the actual configuration attained when a guarded move terminates be X_a, $\mathbf{F}_s$, $\mathbf{P}_s$ and $\mathbf{M}_s$ the sensed force, position and moment in this configuration, and $\mathbf{F}_a$, $\mathbf{P}_a$ and M_a are the actual force, position and moments respectively[6]. Let CF_a be the contact formation in which the motion has terminated. Note that CF_a is a set of configurations and X_a is contained in the set CF_a. Upon termination of the motion, all the velocities and accelerations of all the parts in the assembly (including the robot) are zero. Therefore the system (of parts) is in a *static equilibrium*. If we consider the held object B alone as shown in Figure 7, then the contact forces and moments $\mathbf{F}_i$ and $\mathbf{M}_i$, and, the actual resultant forces $\mathbf{F}_a$ and $\mathbf{M}_a$ must satisfy the static equilibrium conditions. We derive the constraints that must be satisfied by the sensed data, given the object models and uncertainty bounds and current Contact Formation that an assembly is in. We consider separately, the single contact case and the multiple contact case.

Single Contact Cases

Using $F_e = -F_a$ and $M_e = -M_a$ from Fig. 7 the static equilibrium equations (8) and (9) become

$$\mathbf{F}_c + \mathbf{F}_b = -\mathbf{F}_e \tag{16}$$

$$\mathbf{F}_c + \mathbf{F}_b = \mathbf{F}_a \tag{17}$$

$$\mathbf{r}_c \otimes \mathbf{F}_c + \mathbf{M}_c + \mathbf{r}_b \otimes \mathbf{F}_b = \mathbf{M}_a \tag{18}$$

The $\mathbf{F}_a$ and $\mathbf{M}_a$ can never be determined due to sensing errors. We only have an estimate of $\mathbf{F}_a$ and $\mathbf{M}_a$ from the sensed values $\mathbf{F}_s$ and $\mathbf{M}_s$ as in Section 2. Let $\Delta\mathbf{m}$, $\Delta\mathbf{f}$, $\Delta\mathbf{r}_b$ and $\Delta\mathbf{r}_c$ be the difference between the actual and measured quantities. Then

$$\mathbf{r}_c = \mathbf{r}_c^m + \Delta\mathbf{r}_c \tag{19}$$

$$\mathbf{r}_b = \mathbf{r}_b^m + \Delta\mathbf{r}_b \tag{20}$$

$$\mathbf{F}_a = \mathbf{F}_s + \Delta\mathbf{f} \tag{21}$$

$$\mathbf{M}_a = \mathbf{M}_s + \Delta\mathbf{m} \tag{22}$$

Combining Equations 17 and 18 with Equations 19 through 22, we have

[6]It is assumed throughout the thesis that resultant Forces and Moments can be sensed. Typically, such data is sensed using wrist mounted sensors as shown in Figure 7. $\mathbf{F}_s$, $\mathbf{M}_s$, $\mathbf{F}_a$ and $\mathbf{M}_a$ refer to resultant Forces and Moments

$$\underbrace{\mathbf{r}_c^m \otimes \mathbf{F}_s - \mathbf{r}_c^m \otimes \mathbf{F}_b + \mathbf{r}_b^m \otimes \mathbf{F}_b + \mathbf{M}_s}_{\mathbf{L}_1} + \mathbf{M}_c =$$
$$-\mathbf{r}_c^m \otimes \Delta\mathbf{f} - \Delta\mathbf{r}_c \otimes \mathbf{F}_s +$$
$$\underbrace{\Delta\mathbf{r}_c \otimes \mathbf{F}_b - \Delta\mathbf{r}_b \otimes \mathbf{F}_b - \Delta\mathbf{r}_c \otimes \Delta\mathbf{f} - \Delta\mathbf{m}}_{\mathbf{R}_1} \quad (23)$$

All the terms on the right hand side of (23) involve error terms defined above. The left hand side terms ($\mathbf{L}_1$) are known given a hypothesized contact formation. Using the error bounds we can bound the right hand side of (23) and thus produce a test on the hypothesized contact formation. If the test fails, the hypothesized contact formation is incorrect. In practice, this has been found to be a good discriminator.

Now, there are two cases for *single contact*, namely, case of point contact ($\mathbf{M}_c = 0$) and case of *distributed* contact ($\mathbf{M}_c \neq 0$). First, we consider the point contact case, i.e., ($\mathbf{M}_c = 0$); Then by substituting for $\mathbf{M}_c$ in Equation 23 and considering only the x component of the equation, we have:

$$\begin{aligned} L_{1,x} &= -\left(r^m_{c,y}\Delta f_z - r^m_{c,z}\Delta f_y\right) - \left(\Delta r_{c,y}F_{s,z} - \Delta r_{c,z}F_{s,y}\right) \\ &\quad -\left(\Delta r_{c,y}F_{b,z} - \Delta r_{c,z}F_{b,y}\right) + \left(\Delta r_{b,y}F_{b,z} - \Delta r_{b,z}F_{b,y}\right) \\ &\quad -\left(\Delta r_{b,y}\Delta f_z - \Delta r_{b,z}\Delta f_y\right) - \Delta m_x \end{aligned} \quad (24)$$

Equation 24 can be rewritten as following inequality:

$$\begin{aligned} |L_{1,x}| \leq\ & |r^m_{c,y}\Delta f_z| + |r^m_{c,z}\Delta f_y| + |\Delta r_{c,y}F_{s,z}| + |\Delta r_{c,z}F_{s,y}| + \\ & |\Delta r_{c,y}F_{b,z}| + |\Delta r_{c,z}F_{b,y}| + |\Delta r_{b,y}F_{b,z}| + |\Delta r_{b,z}F_{b,y}| + \\ & |\Delta r_{b,y}\Delta f_z| + |\Delta r_{b,z}\Delta f_y| + |\Delta m_x| \end{aligned} \quad (25)$$

From the bounds of the uncertainties and errors we have,

$$\begin{aligned} |\Delta r_{c,y}| \leq \epsilon_u,\ |\Delta r_{c,z}| \leq \epsilon_u \\ |\Delta r_{b,y}| \leq \epsilon_u,\ |\Delta r_{b,z}| \leq \epsilon_u \\ |\Delta f_y| \leq \epsilon_f,\ |\Delta f_z| \leq \epsilon_f \\ |\Delta m_x| \leq \epsilon_m \end{aligned} \quad (26)$$

and

$$\begin{aligned} |L_{1,x}| \leq\ & (\epsilon_f|r^m_{c,z}| + \epsilon_f|r^m_{c,y}| + \epsilon_u|F_{s,z}| + \epsilon_u|F_{s,y}| + \\ & 2\epsilon_u|F_{b,z}| + 2\epsilon_u|F_{b,y}| + 2\epsilon_u\epsilon_f + \epsilon_m) \end{aligned} \quad (27)$$

where

$$\epsilon_u = (2\gamma_p + \epsilon_{pl} + G_p) \quad (28)$$

Desai[29] derives similar constraints for case of a distributed single contact. Denote the contact normal by $\hat{\mathbf{n}}_{c,a}$. Then,

$$\gamma_n|\mathbf{L}_1| - |\mathbf{L}_1 \cdot \hat{\mathbf{n}}_{c,m}| < |\mathbf{R}_1^* \cdot \hat{\mathbf{n}}_{c,m}| + \gamma_n|\mathbf{R}_1^*| \quad (29)$$

where, x component of $\mathbf{R}_1$ is given by,

$$\begin{aligned} R^*_{1,x} =\ & (\epsilon_f|r^m_{c,z}| + \epsilon_f|r^m_{c,y}| + \epsilon_u|F_{s,z}| + \epsilon_u|F_{s,y}| + \\ & 2\epsilon_u|F_{b,z}| + 2\epsilon_u|F_{b,y}| + 2\epsilon_u\epsilon_f + \epsilon_m) \end{aligned} \quad (30)$$

and γ_n is a parameter bounding the error in the deviation of the actual orientation from the modelled orientation, $|\mathbf{n}_a \cdot \mathbf{n}_m| \geq \gamma_n$. Other components can be derived similary.

Desai[29] also derives bounds for the multiple contact case, but they will not be repeated here.

3.3.2 Limitation of Static Verification

Static Verification may fail because, due to errors in sensing and geometry, more than one contact formation may satisfy the constraints. Such a case is depicted in Figure 8. The Contact Formation in Figure 8 (a) may result in the nearly the same values for sensed position, force and moment, as the Contact Formation in Figure 8 (b) if the δ is sufficiently small. We partially circumvent this problem through appropriate design constraints as described in the next section.

Two other situations in which more than one Contact Formation could satisfy the constraints that cannot be prevented by design constraints are shown in Fig. 9 and 10. In the contact situation depicted in Fig. 9, the theoretically sensed moment M_s is zero since we assumed uniform pressure distribution over the contact surface. However, in reality there may be a sensed moment, and the neighboring contact formation depicted in Fig. 9(b) may be verified as satisfying the static equilibrium equation. Similarly, it can be shown [29] that both contact formations in the 2-D situation depicted in Fig. 12 can satisfy the same equilibrium equation. Active verification is used to distinguish contact formations in these cases.

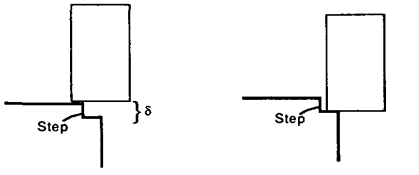

(a) (b)

Figure 8: Contact Formations in (a) and (b) are Indistinguishable because of Uncertainties in sensed data and geometry

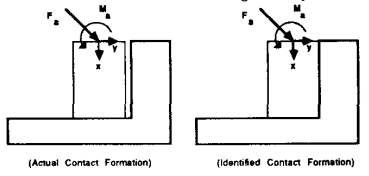

(a) (b)

Figure 9: (a) contact formation, erroneously not identified due to modelling errors, (b) contact formation erroneously identified due to modelling errors.

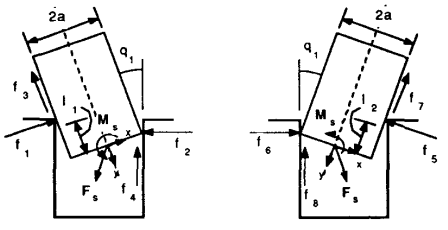

(a) (b)

Figure 10: Indistinguishable Contact Formations for Static Verification Algorithm

3.3.3 Active Verification

The active verification procedure is based on the separation cones that were developed earlier. The basic idea behind active verification is to distinguish among the plausible set of contact formations by generating tests that are known apriori to be true for only one of the contact formations in the plausible set. Then, if the test returns a true the contact formation is uniquely identified. If on the other hand the test returns a false, the contact formation for which the test was generated is eliminated and verification is performed again on the remaining contact formations in the plausible set.

Separation cones can never be exactly determined due to uncertainty with respect to the orientation of the contact plane. However,

we can determine a conservative bound for separation cones for a given contact formation.

In Figure 11 (a) depicts the uncertainty associated with the orientation of the two contact planes cp_1 and cpi_2 for the Contact Formation shown in Figure 4. From the definition of orientation uncertainty we have:

$$\Delta\theta = cos^{-1}\epsilon_o \tag{31}$$

Now, an instantaneous motion in a direction at an angle ϕ_1, such that $0 < \phi_1 < \Delta\theta$ or $\pi - \Delta\theta < \phi_1 < \pi$, where ϕ_1 is measure as shown in Figure 11 (a), cannot be guaranteed to result in separation since we do not know the actual orientation of the contact plane cp_1. Let, $SC_{1,e}$ and $SC_{2,e}$ be the sets of all the directions that are excluded due to uncertainty in orientation for contact planes cp_1 and cp_2 respectively. Then conservative bounds SC_1^* and SC_2^* for the separation cones SC_1 and SC_2 respectively are given by:

$$SC_1^* = SC_1 - SC_{1,e} \tag{32}$$
$$SC_2^* = SC_2 - SC_{2,e} \tag{33}$$

Then, a conservative bound on the actual separation cone for the contact formation is given by:

$$SC^* = SC_1^* \cap SC_2^* \tag{34}$$

The bound on the actual Separation Cone, S^* is shown in Figure 11 (b).

Now, consider the two contact formations CF_a and CF_b for which SC_a and SC_b are the corresponding separation cones and assume for the moment that there is no uncertainty in the orientation of the contact planes. Let $\overline{SC}_a$ denote the complement of set SC_a, i.e, the set of all the directions not in SC_a. Then, if the assembly were in Contact Formation CF_a and a move in any direction d, $d \in \overline{SC}_a$ would not be possible. Now, let direction d such that $d \in \overline{SC}_a$ and $d \in SC_b$. Now, if an instantaneous motion is attempted in d, and if the robot meets more resistance (i.e. the component of sensed force in the direction of the contact plane normal would increase), it would indicate that the assembly is currently in Contact Formation CF_a. If however, when the instantaneous motion is attempted and there is a decrease in resistance (i.e. the component of sensed force in the direction of the contact plane

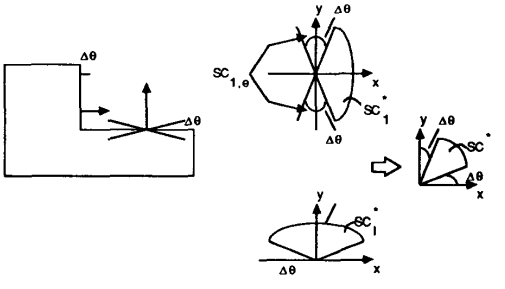

(a) (b)

Figure 11: (a) Uncertainty in Orientation of the Contact Planes (b) Conservative bounds on actual Separation Cone $SC^* = SC_1^* \cap SC_2^*$.

normal decreases), then the Contact Formation must be CF_b. Then, set of directions T_a given by

$$T_a = \widetilde{SC}_a \cap SC_b \tag{35}$$

where
$$\widetilde{SC}_a = \overline{SC}_a - SC_{a,e} \tag{36}$$

is called the *test cone* for contact formation CF_a to distinguish from Contact Formation CF_b. By using CF_a we have now taken uncertainty in the orientation of the contact plane into account. Any direction in set T_a can be used to distinguish contact formation CF_a from contact formation CF_b. The idea of *test cones* can be easily extended to more than two contact formations. Suppose we would like to distinguish a contact formation CF_i in as a set of contact formations $S = \{CF_1, CF_2, \cdots, CF_n\}$, from other contact formations in that set. If $\{SC_1, SC_2, \cdots, SC_n\}$ are the separation cones corresponding to the contact formations in S, then the *test cone* T_i for CF_i is given by,

$$T_i = \widetilde{SC}_i \cap (SC_1 \cap SC_2 \cap \cdots \cap SC_n) = \widetilde{SC}_i \cap \left(\bigcap_{\substack{j=1 \\ j \neq i}}^{n} SC_j \right) \tag{37}$$

Given T_i we can determine if the current Contact Formation is CF_i or not. We use this test as the basis for identification of Contact Formations in *active* verification. The verification algorithm based on a Hypothesis and Testing Scheme is presented in Desai[29].

3.4 Design Constraints and Verifiability

In this section we introduce the notion of design constraints for verifiability. The underlying idea is very simple. If we can identify what causes failure of the algorithms, then perhaps we can select constraints such that those cases do not arise. We will only be considering the single contact cases. To illustrate the need design constraints consider

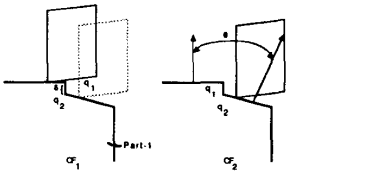

(a) (b)

Figure 12: Indistinguishable Contact Formations: δ and θ are two design parameters for Part–1

the contact formations shown in Figure 12. Let, the hypothesised set of Contact Formations[7] include both CF_1 and CF_2

Suppose that CF_1 is tested for first. Since, CF_1 is the current contact formation, it should pass the *PosContraint* test, which tests if a hypothesised contact formation is plausible given the current sensed position. It should also pass the following test for constraints generated from mechanics. Next, same set of tests are performed for Contact Formation CF_2. Now, by making δ sufficiently small we can ensure that position sensor cannot distinguish between the two Contact Formation (i.e., CF_2 also tests *true* with *PosConstraint*). Next, if θ is nearly equal to zero then it is possible that the computed values for contact forces $\mathbf{F}_1$ and $\mathbf{F}_2$ from the sensed force $\mathbf{F}_s$ and moment $\mathbf{M}_s$ are nearly equal so that constraint from mechanics are satisfied for both the hypothesised contacts. Therefore from static verification point of view CF_1 and CF_2 are indistinguishable. Further, active verification active verification will not be able to distinguish among CF_1 and CF_2 either, because they have nearly identical Separation Cones when θ is equal to zero.

The two Contact Formations shown in Figures 10 can be made distinguishable with respect to each other by appropriate choice of the two parameters, namely, δ and θ, either by increasing the separation between the two surfaces S_1 and S_2 making θ large enough that the force and moment sensors can distinguish between the contact formations.

Design Constraints from Position Sensing

From Figure 12 the contacts at q_1 in CF_1 and q_2 in CF_2 represent the worst case for distinguishability using position sensors alone. If ϵ_p is the uncertainty in position sensing and γ_p is the uncertainty in

[7]For explanation of these terms refer to description of Verification Algorithms in Desai [29].

geometry then circle r_1 centered at q_1 with a radius equal to $(\epsilon_p + \gamma_p)$, marks the boundary within which a point would be indistinguishable from q_1. Then for CF_1 and CF_2 to be distinguishable, δ, should satisfy the constraint:

$$\delta \geq \epsilon_p + \gamma_p \tag{38}$$

Equation 38 represents a design constraint that must be satisfied if contact formations CF_1 and CF_2 have to be distinguishable by position sensing.

Design Constraint from Force Sensing (*Passive*)

Let, $\mathbf{F}_a$ and $\mathbf{M}_a$, and, $\mathbf{F}_s$ and $\mathbf{M}_s$ be the actual and sensed values forces and moments. Reconsidering the two contact formations CF_1 and CF_2 depicted in Figure 12, we note that to differentiate between CF_1 and CF_2 using the force and moment sensors alone, geometric parameters for only one of the contact formations should satisfy the following constraint which arises from static equilibrium considerations:

$$|\mathbf{M}_s - \mathbf{r}_a \otimes \mathbf{F}_a| \leq \epsilon_m \tag{39}$$

The only parameters that we have control over that can differentiate between the two contact formations are the value of $\mathbf{r}_a$ and the direction of force $\mathbf{F}_a$. (Note that the magnitude of the force is not relevant.) If we impose no restrictions on $\mathbf{r}_a$ for the two contact formations (i.e., no constraint on value of δ), then direction of contact forces that arise for CF_1 and CF_2 should be such that the constraint in inequality 39 is satisfied for only one of the contact formations.

When, friction is present the contact force may be in any direction within the friction cone. Additionally, due to the uncertainty in orientation, the direction of the friction cone axis is also unknown within some uncertainty cone due to modelling error. Further, the normal of a surface is found by the sensed direction of the force $\mathbf{F}_s$. Thus, there are three components leading to the angular uncertainty. By choosing a sufficiently large applied force it is possible to reduce the relative effects of sensor errors. However, practical considerations limit us from using any arbitrary value for applied force. Let F_{min} be the minimum force applied. Then error in estimating the angle of the normal is given by:

$$\Phi_s = sin^{-1}\frac{\epsilon_f}{F_{min}} \tag{40}$$

The angle of the friction cone is given by $\Phi_\mu = tan^{-1}\mu$ where μ is the coefficient of friction. Further since we modelled the error limit in modelling error by $|\mathbf{n}_m \cdot \mathbf{n}_a| \geq \gamma_u$, the maximum error from modelling is $\Phi_u = cos^{-1}\gamma_n$ Then, the design constraint becomes,

$$\theta \geq 2(\Phi_s + \Phi_u + \Phi_u) \tag{41}$$

$$\theta \geq 2\left(cos^{-1}\gamma_n + tan^{-1}\mu + sin^{-1}\epsilon_f\right) \tag{42}$$

The factor of two arises because there are two surfaces we are trying to distinguish and θ must exceed the run of their uncertainties.

Desai[29] has shown that the design constraints from active serving are less restrictive than those derived here.

In summary, we can state two design constraints: 1) A minimum distance (δ) given by Equation 38 must be maintained between any two surfaces that are parallel or nearly parallel (i.e., do not satisfy the other constraint). 2) The surface normals of two adjacent or nearly adjacent surfaces must satisfy the angular separation condition given by Equation 42.

4 Conclusions

Our long term goal is to discover reasonable constraints under which an automatic uncertainty handling strategy (for robot part-mating tasks) is guaranteed to succeed. As the first steps in this direction, we have developed the concept of contact formation and techniques for determining the contact formation in which a pair of parts together with the design constraints sufficient to guarantee the success of the verification algorigthms. The verification algorithms presented here have been implemented on an assembly system consisting of a PUMA robot, RTI sensors and a Apollo workstation. The algorithms were tested for simple assembly operations such as peg in hole. The experiments are described in Desai [29].

References

[1] R.A. Brooks and T. Lozano-Perez. A subdivision algorithm in configuration space for findpath with rotation. *IEEE Trans. on SMC*,

[2] T. Lozano-Perez and M. Wesley. An algorithm for planning collision-free paths among polyhedral obstacles. *Comm. ACM*, 22(10):560–570, October 1979.

[3] T. Lozano-Perez. *Automatic planning of manipulator transfer movements.* Artificial Intelligence Lab, MIT, December 1980.

[4] J. Barber, R. Volz, R. Desai, R. Rubinfeld, B. Schipper, and J. Wolter. Automatic evaluation of two-fingered grips. *IEEE Journal of Robotics and Automation*, RA-3(4):356–361, August 1987.

[5] M. R. Cutkowsky. *Robotic Grasping and Fine Manipulation.* Kluwer Academic Publ., Boston, 1985.

[6] M. T. Mason. Manipulator grasping and pushing operations. In M. T. Mason and J. K. Salisbury, editors, *Robot Hands and the Mechanics of Manipulation*, pages 171–298, MIT Press, Cambridge MA, 1985.

[7] J.D. Wolter, R.A. Volz, and A.C. Woo. Automatic generation of gripping positions. *IEEE Trans on Systems, Man and Cybernetics*, SMC-15(2):204–213, March 1985.

[8] M. Gini. Symbolic and qualitative reasoning for error recovery in robot programs. *Int. NATO Workshop*, 1986.

[9] R. H. Taylor. *The synthesis of manipulator control programs from task-level specifications.* Artificial Intelligence Lab, Stanford Univ., July 1976.

[10] R.A. Brooks. Symbolic error analysis and robot planning. *International Journal of Robotics Research*, 1(4):29, 1982.

[11] B. Dufay and J. C. Latombe. An approach to automatic robot programming based on inductive learning. August 1983. unpublished.

[12] T. Lozano-Perez, M. T. Mason, and R. H. Taylor. Automatic synthesis of fine-motion strategies for robots. *The International Jour. of Robotics*

[13] M.T. Mason. Automatic planning of fine motions: correctness and completeness. *Int. Conf. on Robotic*, 492–503, March 1984.

[14] M. Erdmann. Using backprojections for fine motion planning with uncertainty. *The Int'l Journal of Robotics Research*, 5(1):19–45, 1986.

[15] B.R. Donald. Robot motion planning with uncertainty in the geometric models of the robot and environment: a formal framework for error detection and recovery. *Proc. IEEE Int. Conf. on Robotics and Automation*, 1588, 1986.

[16] D.E. Whitney. Historical perspective and state of the art in robot force control. *Proc. IEEE Int. Conf. Robotics and Automation*, 262, March 1985.

[17] O. Khatib and J. Burdick. Motion and force control of robot manipulators. *Proc. IEEE Int. Conf. Robotics and Automation*, 1381, 1986.

[18] M. T. Mason. Compliance and force control for computer controlled manipulators. *IEEE Trans. on Systems, Man, and Cybernetics*, SMC-11(6):418–432, June 1981.

[19] M. H. Raibert and J. J. Craig. Hybrid position / force control of manipulators. *ASME Jour. of Dynamics Systems, Measurement and Control*, 102:126–133, June 1981.

[20] D. E. Whitney. Force feedback control of manipulator fine motion. *ASME Jour. of Dynamic Systems, Measurement and Control*, 126–133, June 1977.

[21] R.C. Brost. Automatic grasp planning in the presence of uncertainty. *Proc. IEEE Int. Conf. on Robotics and Automation*, 1575, 1986.

[22] M. Erdmann and M. T. Mason. An exploration of sensorless manipulation. *Proc. IEEE Int. Conf. on Robotics and Automation*, 1569, 1986.

[23] M.A. Peshkin and A.C. Sanderson. Planning robotic manipulation strategies for sliding objects. *Proc. IEEE Int. Conf. Robotics and Automation*, 696, 1987.

[24] M.T. Mason. Compliant motion. 1982. unpublished.

[25] R. Desai. On fine motion in mechanical assembly in presence of uncertainty. *Ph.D. Dissertation*, 1988.

[26] J.J. Kalker. Numerical contact elastostatics. *Preprint of paper presented at Euromech Colloquium No. 110 Contact Problems and Load Transfer in Mechanical Assemblages*, September 1977.

[27] T. Torigaki and N. Kikuchi. Finite element stree analysis of a class of three dimensional contact problems with friction. *Canadian Conference on Industrial Computer Systems*, May 1984.